Alexandria Engineering Journal (2023) 64, 833–846

HOSTED BY

Alexandria University

Alexandria Engineering Journal

www.elsevier.com/locate/aej
www.sciencedirect.com

# Structural analysis and optimization of machine structure for the measurement of cutting force for wood

Aditya Sharma [a], Sashank Thapa [a], Bhaskar Goel [a], Raj Kumar [a], Tej Singh [b,*]

[a] Faculty of Engineering and Technology, Shoolini University, Solan, Himachal Pradesh 173229, India
[b] Savaria Institute of Technology, Faculty of Informatics, ELTE Eötvös Loránd University, Szombathely 9700, Hungary

Received 2 July 2021; revised 30 August 2022; accepted 13 September 2022
Available online 24 September 2022

**KEYWORDS**

Computer aided engineering;
Structural optimization;
Additive manufacturing;
Computer numeric control;
Topology;
Hypermesh

**Abstract** Structural Integrity and its response to the subjected cutting forces during machining, plays a vital role in the performance and the life of the machine tool. The machine tool must meet the demands of the stiffness and easy maintenance; in absence of this the desired machining accuracy during cutting operation is not achieved. While at the same time the machine structure cannot be made heavy which increases the manufacturing cost. The use of stiffener plates is a solution to this problem. However, the selection of the appropriate locations of stiffener plates based on only designer's design knowledge and experience may not lead to desired results. Hence, Structural analysis in conjunction with the structural optimization methods are employed for getting optimized structures. In this paper, experimental results obtained from the cutting force measuring machine which was manufactured for the experiment were used to analyse and optimize the structure of machine tool. The analysis and optimization were done with the help of Finite element methods technique (Optistruct solver) and modelling being done in Hypermesh. The optimized structure with stiffeners, led to the decrease in the maximum displacement thus increasing the stiffness of the machine structure while avoiding resonance.



## 1. Introduction

Static and dynamic stiffness are crucial parameters in machine tool construction. The machine's output, accuracy, and speed are all affected by these parameters. This means that the design of the machine itself has a negative impact on its efficiency [1,2]. When it comes to high-precision machining, a problem that has recently emerged is the dynamic nature of machine tools, particularly vibration brought on by a lack of rigidity. Many researchers have examined the issue of machining error caused by the reduced rigidity of the machine frame and concluded that it is a significant barrier to achieving precise machining [3–5]. Machine tools during manufacturing processes, faces many issues due to weight of its own assembled components, handling and operating large volumes of

* Corresponding author.
E-mail address: sht@inf.elte.hu (T. Singh).
Peer review under responsibility of Faculty of Engineering, Alexandria University.

https://doi.org/10.1016/j.aej.2022.09.030
1110-0168 

material, and forces due to dynamic loading caused during cutting operations. This causes several problems, including stresses, strains, resonance, chatter, etc. For the sake of safety and extending the machine tool's lifespan, it is essential to maintain these stresses and strains below the permissible limits. To prevent machine tool failure and regular maintenance expenses, the machine tool's design and material must be carefully chosen. The research carried out by numerous researchers makes the significance of the material choice obvious [6–8].

Since the structure's configuration significantly affects the machine tool's dynamic properties, it's important to investigate it early in the design process. Conversely, only few manufacturers make use of advance technology and instruments to check out different design configurations due to its high cost involved and large time consumption. Therefore, there is a need for easy-to-use and dependable simulation software to avoid these problems. The two main examples of simulation approaches for machine tools are the finite element method (FEM) and the rigid multi-body simulation (MBS) [9]. The FEM is a popular and commonly used model in industry. Several researches have been carried out using the FEM to model machine components [10]. Experimental evaluation for stability of cutter blade in ANSYS (Analysis of systems) revealed that machine structure design played a significant role in it [11]. Other different research in FEM software [12–14] has revealed that the structural design and optimization is a crucial component for cutting tool stability and the reduction in mass and volume. Lightweight and high stiffness designs are possible with the help of the careful and judicious use of the optimization methods [15]. It is possible by elimination of the redundant elements leading to reduction in the material utilized to a great extent [16]. Design is motivated by the designer's intent, the purpose for which the machine is made. The decisions are based on the resources' availability, cost, and need. In order to get the desired results, a good design must employ the fewest resources possible. The right material must be chosen and used to its full potential when the machine's design is cost constrained. They can be accomplished via the material choice, structural design, and CNC machine tool control system [17]. Today, a large range of materials, including steels, cast irons, and reinforced composite materials, are available. Additionally, there are currently new intelligent and smart materials on the market that have sensors and actuators. Due to the costs involved in such alterations, it might not always be possible to replace the material totally [18]. The utilization of components like ribs is beneficial when lightweight components and material cost are important in product development. The machine tool construction is made stiffer by the inclusion of ribs. To determine a rib pattern's appropriateness and ability as a machine component, a thorough investigation of the various rib patterns is necessary [19]. Even when the designer's expertise and analytical research produce well-calculated outcomes, it could not be the ideal answer. To make the machine more flexible and less redundant, it is preferred that the location of these components be determined by the loads that machine is experiencing. This issue might have a solution in topology optimization. It is the kind of structural optimization that is most versatile. To achieve the specified purpose, it seeks to identify the ideal material distribution within the design area. It satisfies the greatest design purpose, which may be followed by design fine-tuning to provide other design improvements [20,21].

### *1.1. Machine tools and cutting forces in wood*

Research on evaluating the mechanical characteristics of wood has been ongoing for a long time. Numerous techniques have been employed to assess the orthotropic characteristics of wood. To estimate these parameters many researchers has used an off-axis tension test using digital image correlation experiments [22]. A few non-destructive techniques have also been used on culturally significant specimens [23]. The anisotropic property of wood causes the variance in cutting force. According to research on the handsaw's cutting mechanism for woodworking, the mechanism for cutting across and along the grain is different [24]. The many cutting processes include bending, shearing, and chiseling. Therefore, proper consideration is needed while calculating cutting forces. Dynamometers are frequently employed to determine these forces. The studies were carried out for cuts of varying depths on the same workpiece as well as cuts of the same depth on several workpieces which revealed that in terms of tool life and power usage, cutting force is crucial [25–27]. It was also found that the variation in estimated angle between tangential and cutting force affects tool wear [26]. For determining the cutting force, there are other additional techniques, such as density models and mechanical features. The best explanation for wood machining was found due to the elastic nature of wood [28]. Wood, it seems from what we were able to determine from our literature review, is a highly anisotropic material, with material qualities varying in each direction of grains. Species differ in their ability to cut because each has its own unique mechanical feature; this makes the cutting operation non-homogeneous and makes the prediction of cutting force difficult. CNC machine used for carving of wood is now days modeled using finite element analysis (FEA), and the results are reviewed, analyzed, and optimized based on the tasks they will do. The input parameter in design of these wood carving CNC machines starts from the cutting force which the system should withstand. Additionally, analytical techniques for component selection and stability calculation are investigated using the cutting force. The necessity for calculating cutting forces of wood is due to manufacturing of light weight CNC machines for carving in different woods.

### *1.2. Structural analysis and topology optimization*

Analysis, both static and dynamic, is essential for determining how machine tool structure behaves. These analyses have been used in many different types of research to forecast how machine tools will perform [29–32]. For example, in the study of the optical aspherical machine [30], it was discovered that the stiffness was significantly lower in the horizontal than in the vertical direction for the grinding process. The ram (z-axis guideway) when subjected to modal analysis, the initial natural frequency was discovered to be greater than twice that of the maximum spindle speed [30]. Numerous other studies have carried out on structural analyses of lathe beds [29], tool beds [33], and CNC router [34]. One of the latest engineering design methodologies, structural optimization has helped to create new products with increased stiffness and reduced weight. Structural optimization can be classified into three categories namely topology, size, and shape optimization based on the type of design variables. Size optimization is used when the shape and topology of the structure are known. The thickness of the members is treated as the design variable. Shape optimization, on the other hand, is used when the topology of the structure is known and one must find the appropriate shape of geometry like the holes, fillets, etc. Topology optimization is used to find appropriate material topology that fulfills the given design criteria. These three categories of optimization refer to different stages of the design process [35]. Topology optimization, also known as the conceptual design, is followed in early design stages. Size and shape optimization are collectively known as design fine-tuning that is used in later stages of the design cycle [36]. It was also found from previous study that few researchers have employed these three optimizations' techniques in a single step. This helps in maximum utilization of design space and leads to better results [37–40]. Topology Optimization is one of the latest optimization techniques and is one of the best option for the creation of innovative products [41]. The use of these techniques has been widely appreciated in many industries including aeronautics, automotive etc. [42]. The advances in the field of additive manufacturing have encouraged the use of optimization in various fields. For instance, topology optimization with Additive Manufacturing (AM) was used for the creation of the module of a humanoid robot. The robot was designed for football championship for which mobility and hence low weight was the design objective. Topology optimization was done for three different materials and was manufactured using AM. It was found that the topology optimized parts were better in strength as compared to the initial design. However, Aluminum alloy offered more advantage due to its low weight even outperforming the initial component load bearing capabilities with similar material properties [43]. Topology optimization problem may be based on many different optimization methods [44]. The research carried out by using three different software for an optimization problem with same loads, materials, and constraints, it was found out that due to different algorithms used by these software's they obtained different final topologies. The differences in them being the way they treat the design domain [45]. The topology optimization is classified into two groups: soft skill and hard skill methods. Soft skill methods allow for partial material densities whereas ESO (Evolutionary Structural Optimization) which is a hard skill method iteratively removes or adds a finite amount of material. The soft skill methods like level set methods; soft skill options (SKO) and evolutionary algorithms (EA) require further research to be more acceptable as design tool. It was found that Solid Isotropic Microstructure with Penalization (SIMP) which is one of the soft skill methods is the most researched and implemented method. The effectiveness of this method has been proven by various researches done in the field of structural optimization. SIMP topology optimization technique was used for the optimization of a perforated beam web opening. It was found that the topology optimized design performed better at stiffness, shear buckling load and yield load [46]. The optimization's value as a design tool has been confirmed by several researchers. One of the researchers optimized the lathe bed using ANSYS software. To confirm that the optimized section functioned better than the original bed, they used the Finite Element Method (FEM) to do static and dynamic analysis. Topology optimization requires the selection of suitable constraints. On the topology optimization problem, it was discovered that manufacturing constraints lead to greater compliance values. The type of manufacturing process, size, and shape all affect how the manufacturing constraints are implemented; however, this kind of constraint is not necessary because optimal solutions typically form self-supporting structures [47,48]. From the literature review it has been found that although topology optimization is the effective tool for machine structure manufacturing, but a very few literatures related has found to use it with dynamic loading conditions of cutting tool operation for avoiding bending stiffness in structure to achieve high machining precision. Secondly the conjunction of structural analysis and optimization simultaneously using FEM (Hypermesh and Optistruct) software is today's design requirement. In the present work, topology optimization is used for finding best topology under the given set of the load conditions for which the cutting force measuring machine has been designed specifically because in many studies the actual loading is not involved in analysis as found. The optimal topology finally obtained for cutting force measuring machine was compared with originally fabricated structure to see the effect of the design modifications using FEM. Also, the present research is based on energy method for measurement of force, which can be further advanced to measure actual cutting force measurement without providing any compensation considering the flexibility of the workpiece. In many cases, traditional direct measuring devices cannot be used because they would disrupt the cutting process. Both the cutting forces and the surface roughness are nonlinear with increasing cutting tool diameter. The response characteristics are highly sensitive to the diameter of the tool. In energy method the tool diameter factor is not required. The product available in market such as Lathe Tool Dynamometer, Piezoelectric force measuring systems etc., for cutting force measuring operations start from 5 to 6 times costlier than current proposed model in this study. The present research is a step to fabricate indigenous cutting force measuring machine which apart from measuring the cutting force combined apply the topology optimization on the structure against these forces. There are several other methods for indirect calculation of cutting forces like chip thickness accumulation, Mathematical modelling of flexibility matrix etc., but these requires further processes like scanning electron microscope testing and other validation techniques. Topology optimization is used in the initial phase of the design to which is obtained from the functional specifications to optimally distribute material inside the available volume of a structure. Also, it has the biggest optimization potential and thus a major influence on the behaviour of the final structure and its quality of response. Conceptually, topology optimization is a mathematical technique used in design development. This strategy was developed to distribute the available resources more evenly across the model. A design is generated by the programme considering the designer's constraints, the applied load, and the available space. To put it simply, topology optimization is the process of making a design space out of a 3D model. To make the design more effective, it then eliminates or relocates internal components. The novelty of the present work is that the method is suitable for mini and micro industries and research for modelling and manufacturing of small CNC machines for wood carving, where the present research work provides two important inputs i.e., cutting force data and topology optimization. The present study is helpful for designers, manufacturer, and researchers to design and modify the new and existing machine tool structure and its fabrication using this approach at low cost and simple in calculation.

## 2. Methodology

Machine tools are subjected to high vibration during cutting operation. Therefore, it requires high static and dynamic stiffness. The objective of current investigation is to find appropriate topology for stiffener plates avoiding resonance condition. The cutting force calculated from experimental results is used for the topology optimization and structural analysis for design validation.

### *2.1. Experimental analysis for finding the cutting force*

The cutting experiments were performed in the two directions perpendicular and parallel to the grain for the wood. Five wood samples were chosen for the analysis: Teak, Deodar, Mindi, Sheesham and Sal wood. In which two are softwoods (Mindi and Deodar) and three are hardwoods (Teak, Sheesham and Sal). A constant feed rate of 714 mm/min was used for the experimentation. Wood is orthotropic in nature which leads to variation in the cutting force in the three perpendicular directions. The cutting force was investigated in two directions. Five observations were taken for each wood in tangential and radial directions for investigation to see the variation of cutting force in these two directions. Fig. 1 shows the three views of cutting force measuring machine. The workpiece is held in G-Clamp. The scissor jack is used for feed whereas cutting power is provided by the motor. A 180 W AC motor is installed in the machine. Voltammeter displays the reading of the current and voltage supplied to the motor.

Table 1 and Table 2 give the cutter specifications for the experimental investigation of wood and information about the wood samples, respectively.

The aluminum sample was also investigated using a similar experimental setup with parting wheel as the cutting tool. An L-shaped specimen (25 mm × 25 mm × 2 mm) was used. The cutting was done perpendicular to the cross-section of the workpiece. Table 3 gives information about the cutter specifications.

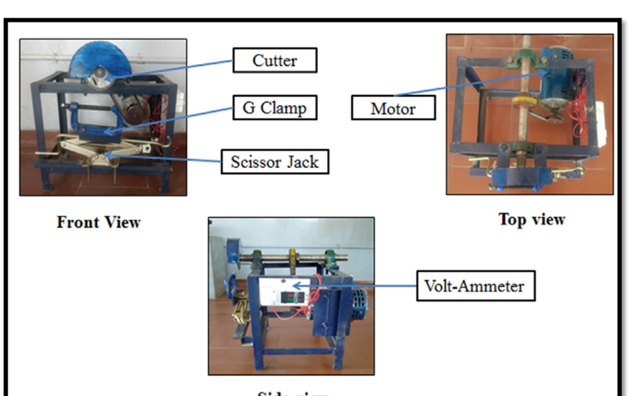


**Fig. 1** Front, top and side view of the cutting force measuring machine.

**Table 1** Cutter specifications for experimental investigation of wood.

| Cutter type | Circular Saw |
|---|---|
| Cutter material | Aluminum body with titanium cutter teeth |
| Number of teeth | 40 |
| Cutter diameter | 102 mm |

**Table 2** Specimens used for wood cutting.

| Wood | Dimensions (mm) | Moisture Content by weight (%) |
|---|---|---|
| Teak | 150 × 50 × 20 | 9.19 % |
| Sal | 150 × 50 × 20 | 12 % |
| Mindi | 150 × 50 × 20 | 13.78 % |
| Deodar | 150 × 50 × 20 | 8.28 % |
| Sheesham | 150 × 50 × 20 | 10 % |

**Table 3** Cutter specifications for experimental investigation of metal.

| Cutter type | Parting wheel |
|---|---|
| Cutter material | Aluminum oxide |
| Cutter diameter | 102 mm |

### *2.2. Finite element model of the machine*

The finite element model of the machine tool was prepared in Hypermesh. The model was based on three assumptions. Firstly, the machine was fixed at bottom and not allowed to move in any direction. Secondly, all the components of the model were homogeneous and isotropic. Lastly, motor was replaced by a concentrated point mass placed at its centre of gravity. Centre of gravity of the motor was calculated by careful examination of the geometry of the motor.

#### *2.2.1. Materials and loads*

Machine tool structure, scissor jack, bearing housing, spindle was made up of mild steel, alloy steel, cast iron and mild steel respectively. The cutter was made up of aluminum with titanium teeth. G-clamp and pulley material was taken as cast iron. Two loading cases were setup one considering the static load and other considering the dynamic cutting forces. The loads were applied to the workpiece and on the cutter teeth in contact with the workpiece. The force was uniformly distributed between the cutter teeth in the direction tangential to the cutter. The loads were variable as cutting forces vary with the wood and direction of cutting. Hence, the maximum force that was experienced during the experimentation was treated as the load for the current analysis. Fig. 2 shows mesh strucure with loading and boundary conditions with mesh element.

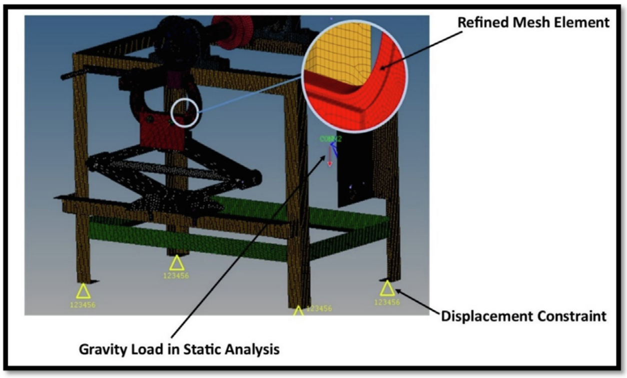


**Fig. 2** Finite element model of cutting force measuring machine.

*2.2.2. Geometric constraints*

The constraints were applied on machine tool to restrict the motion of the machine tool structure. The feet of the structure were assumed to be fixed in all three directions not allowing any movement in any direction.

*2.2.3. Element size*

Element size plays a very important role in the structural analysis. Element size must be sufficiently small for required accuracy on the solution. Smaller size elements, however, increase the solution time. Average element size of 1.5 mm was used. Hexahedral solid elements were used for three dimensional components whereas quad shell elements were used for two dimensional structures. Machine tool structure is modeled by quad shell elements while all other components by hexahedral elements. The number of pentahedral and triangular elements which comes with the hexahedral element was kept below 4 %. Rigid elements, RBE2 were used to connect mass element CONM2 i.e., motor with machine frame. Sixteen elements were used for modeling the hole. The local mesh refinement was done to have stress results with accuracy of $\pm 0.001$ N/mm$^2$. Table 4 shows the types of elements for the present FEM analysis.

*2.3. Finite element analysis*

The FEA analysis was done with the help of Optistruct software. Three different analyses were performed using the similar constraints. First, linear static analysis was done by considering the body forces only. No loads whatsoever were acting on the machine except gravity. The static analysis reveals the stresses setup in machine tool due to the body weight of machine and its components. Then a linear dynamic analysis was performed by considering the dynamic forces i.e., cutting forces. It was assumed that the cutting forces act tangential to the cutter. The cutting forces were applied on the cutter as well as the workpiece. It helps us to find the nature and type of stresses acting on different components while cutting. Lastly, a modal analysis was done to reveal the different modes of vibration and check for condition of resonance. The rated motor rpm was found to be 1440, which was verified with the help of a tachometer. However, the rpm was variable during cutting, the minimum being 1330. The former was considered for analysis and evaluation. The frequency of the motor was hence calculated to be 24 Hz from Eq. (1). For safety, $24 \pm 10$ Hz frequencies of the structure were restricted during optimization.

**Table 4** Type of element for FEM analysis.

| Type of elements | Element information | Value |
|---|---|---|
| Quad shell elements | Number of nodes | 73,561 |
| | Number of elements | 71,422 |
| Hexahedral solid elements | Number of nodes | 398,620 |
| | Number of elements | 303,484 |
| Rigid body elements | Number of nodes | 42 |
| | Number of elements | 1 |
| Mass element | Number of elements | 1 |

$$f = \frac{N}{60} \quad (1)$$

Where, $f$ is the frequency of the motor in Hz or cycles per second and N is the rpm of the motor.

*2.4. Topology optimization*

Appropriate location of the stiffener plates in the machine tool structure used depends upon the experience and design knowledge of engineer. The design hence obtained was good, but it would be difficult to achieve the best results under given load conditions. Topology optimization, however, is a powerful tool in these types of uncertain conditions. The initial dimension of the machine tool structure as shown in Fig. 3, the dimensions of the machine tool structure are in millimeters. Topology optimization helps in finding the right material distribution that would satisfy the given constraints under given load conditions. The objective of the current problem was to maximize the displacement stiffness of the machine tool structure. Hence, compliance minimization was treated as the objective of the given problem. The constraints were provided on the volume of the structure and natural frequencies of the sys-

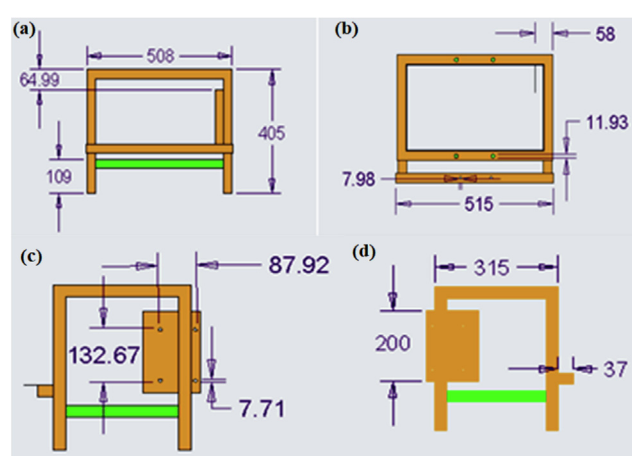


**Fig. 3** Initial dimension of machine tool structure of cutting force measuring machine.

tem. The mass constraint was fixed to 35 % of the initial volume. Natural frequencies ranging from 14 to 34 Hz were constrained. Also, manufacturing constraints of minimum member size of 25 mm were applied to the problem. The Fig. 4-a-b gives the methodology that was used in the current investigation and pictorial representation of the steps.

The mathematical expression for the minimum compliance optimization is given in Eq. (2).

$$\begin{aligned} \text{Minimize : } C(x,u) &= \tfrac{1}{2}u^T K u \\ subjectto: Ku &= f \\ V(x) = \int_\Omega x d\Omega &\le Vc \end{aligned} \tag{2}$$

Where, C(x, u) is the global compliance, K is the global stiffness matrix, x is the density vector, u and f is global displacement and global load vector, Ω is the design domain; Vc is the volume constraint [35]. Optistruct uses the SIMP optimization method for the Topology optimization. It allows the material densities to have fractional densities from 0.001 (least important) to 1 (most important) for any given location in design domain. It informs the designer which parts are necessary and one that can be eradicated. The fractional densities are multiplied with the young's modulus using a suitable penalization factor for getting modulus values at any given location given by Eq. (3) and Eq. (4):

$$0.001 \le x_i \le 1 \tag{3}$$

$$E(x) = x^p E_0 \tag{4}$$

Where, $x_i$ is local density vector, p is the penalization factor, $E_0$ is absolute value of young's modulus and $E_p$ is Young's modulus at any given location [35,49]. Additional constraints on frequency were applied as given below in Eq. (5).

$$\omega_i \le \omega_n \le \omega_j \tag{5}$$

The $\omega_n$ is the circular natural frequency of $n^{th}$ mode; $\omega_i$ and $\omega_j$ are the upper and lower limits of the restricted circular natural frequencies. It is calculated through modal analysis, by solving the free vibration equation as given in Eq. (6). The solution of which is given in Eq. (7).

$$M\ddot{x} + Kx = 0 \tag{6}$$

$$\left(K - \omega_n{}^2 M\right)\Psi_n = 0 \tag{7}$$

Where M is the mass matrix, K is the global stiffness matrix, $\ddot{x}$ and × is the acceleration and displacement vectors; $\Psi_n$ is the Eigen vector or mode shape of $n^{th}$ mode [32,50].

## 3. Results

### *3.1. Experimental analysis for finding the cutting force*

Experimental investigation of wood cutting on the machine was done to determine realistic loads acting on the machine tool structure. The difference in power utilized by machine during cutting and idle condition was used for the estimation of the cutting force. The power developed by motor is calculated by Eq. (8).

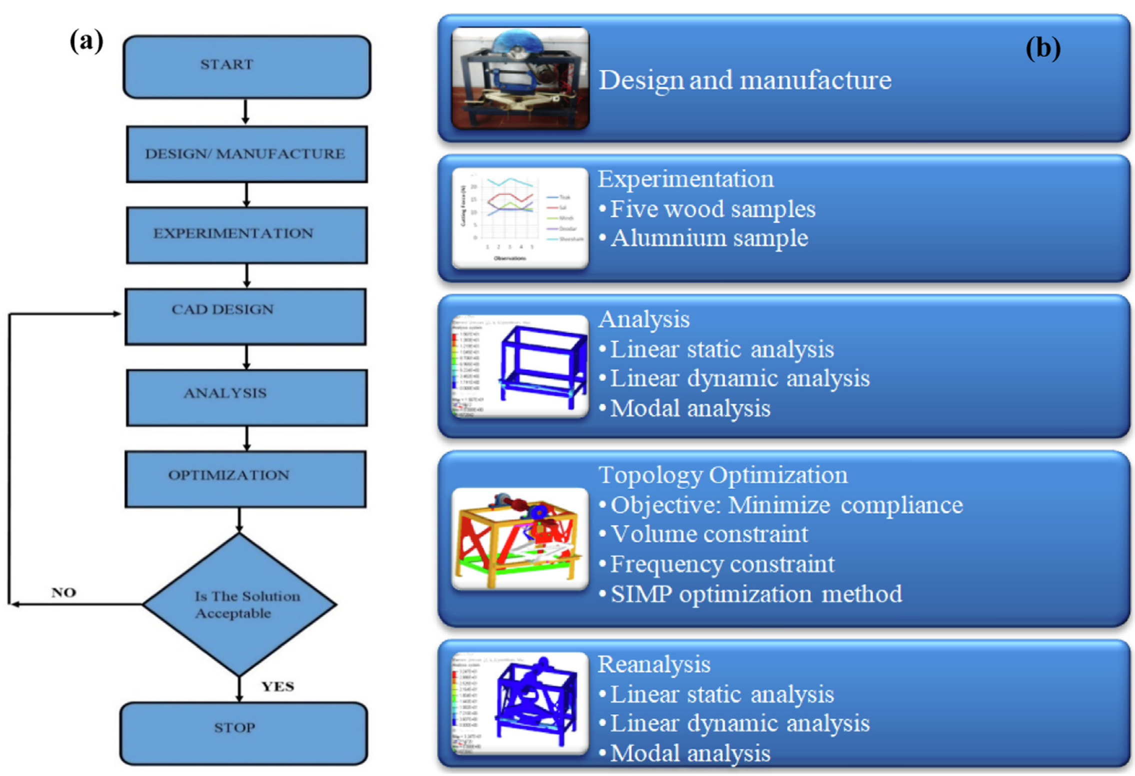


**Fig. 4** (a) Methodology followed in the present work, and (b) Pictorial view.

$$P = VICos\Phi \tag{8}$$

Where P is the power developed by motor in Watts, V is the Voltage in volts, I is the Current in amperes and Φ is the phase angle between voltage and current. Cos Φ is termed as power factor, measure of true power absorbed by the motor. The true power developed by the motor is a function of the motor power factor. It is zero at no load condition [51]. Hence, suitable power factor correction factor must be applied to estimate the power output [52,53]. However, the power factor of the single-phase domestic motor is low in comparison to the three-phase motors used in industries [54]. It was assumed that the power factor variation with load is linear. This assumption is good for estimation of power factor at loads greater than 50 % of full motor output. However, at lower loads the relation between the two is highly non-linear which gives inaccurate power factor values and hence cutting force values may be incorrect. The power factor for the motor was calculated to be variable from 0.16 to 0.248 for half and full loads respectively [55]. The cutting force was calculated from equation (10), and the maximum value was used further in analysis and optimization results that were obtained being given in Tables 5-9.

$$T_{lb-ft} = \frac{P \times 7.043}{N} \tag{9}$$

$$F_C = \frac{T_{lb-ft} \times 1.356}{r} \tag{10}$$

Where $T_{lb\text{-}ft}$ is the calculated torque in lb-ft, N is speed of motor in rpm, r is the radius of cutter in mm and Fc is cutting force in Newton. Torque is a direct function of the power developed by the motor and rpm of the motor. As the rpm of the motor does not vary much during the process of cutting, torque is mainly dependent on the power delivered by the motor. The cutting force delivered is a function of cutter diameter and torque, but the cutter diameter is same in all cases. This implies that the cutting force is primarily the function of the power delivered by motor only.

The cutting force was calculated for different wood samples along the tangential and radial directions. It was found that the cutting force required for cutting was not only dependent on the material but also on the direction of cutting for wood. It is due to orthotropic nature of wood. The cutting force however, for the aluminum remained same along all directions. Hence, it was not found necessary to conduct the experiment in different orientation of workpiece. Table 5 and 6 shows the values calculated of cutting forces for softwood in tangential and radial direction, Table 7 and 8 shows the values calculated of cutting forces for hardwood in tangential and radial direction and Table 9 shows the value of cutting force for Aluminum.

It was seen that the maximum cutting force was found for cutting of aluminum which was equal to 25.436 N. It was also observed that in this case motor was running at full load i.e., 180 W. It is the maximum cutting power the machine tool could deliver, maximum loads that it will ever encounter while

**Table 5** Cutting forces estimation for softwood in tangential cutting.

| Wood | Observation | Cutter speed (rpm) | Cutting power (W) | Cutting force (N) |
|---|---|---|---|---|
| Mindi | 1 | 1372 | 101.205 | 14.12 |
| | 2 | 1387 | 81.432 | 11.20 |
| | 3 | 1383 | 100.34 | 13.92 |
| | 4 | 1372 | 80.388 | 11.20 |
| | 5 | 1375 | 81.432 | 11.28 |
| Deodar | 1 | 1374 | 98.1775 | 13.70 |
| | 2 | 1374 | 81.420 | 11.30 |
| | 3 | 1361 | 80.736 | 11.30 |
| | 4 | 1380 | 80.388 | 11.14 |
| | 5 | 1378 | 100.340 | 13.96 |

**Table 6** Cutting forces estimation for softwood in radial cutting.

| Wood | Observation | Cutter speed (rpm) | Cutting power (W) | Cutting force (N) |
|---|---|---|---|---|
| Mindi | 1 | 1372 | 65.136 | 9.06 |
| | 2 | 1398 | 65.964 | 9.02 |
| | 3 | 1387 | 40.832 | 5.62 |
| | 4 | 1372 | 63.756 | 8.88 |
| | 5 | 1375 | 64.584 | 8.98 |
| Deodar | 1 | 1387 | 84.564 | 11.64 |
| | 2 | 1391 | 65.964 | 9.06 |
| | 3 | 1361 | 80.736 | 11.32 |
| | 4 | 1380 | 63.756 | 8.82 |
| | 5 | 1378 | 64.032 | 8.88 |

**Table 7** Cutting forces estimation for hardwood in tangential cutting.

| Wood | Observation | Cutter speed (rpm) | Cutting power (W) | Cutting force (N) |
|---|---|---|---|---|
| Teak | 1 | 1382 | 63.480 | 8.76 |
| | 2 | 1385 | 80.040 | 11.00 |
| | 3 | 1382 | 79.344 | 10.92 |
| | 4 | 1384 | 76.692 | 11.00 |
| | 5 | 1386 | 75.7045 | 10.50 |
| Sal | 1 | 1387 | 84.564 | 11.64 |
| | 2 | 1391 | 65.964 | 9.06 |
| | 3 | 1361 | 80.736 | 11.32 |
| | 4 | 1380 | 63.756 | 8.82 |
| | 5 | 1378 | 64.032 | 8.88 |
| Sheesham | 1 | 1360 | 162.489 | 22.84 |
| | 2 | 1348 | 145.314 | 20.60 |
| | 3 | 1330 | 162.489 | 23.34 |
| | 4 | 1350 | 152.668 | 21.64 |
| | 5 | 1350 | 144.072 | 20.36 |

**Table 8** Cutting forces estimation for hardwood in radial cutting.

| Wood | Observation | Cutter speed (rpm) | Cutting power (W) | Cutting force (N) |
|---|---|---|---|---|
| Teak | 1 | 1389 | 64.310 | 8.84 |
| | 2 | 1391 | 66.516 | 9.14 |
| | 3 | 1382 | 79.344 | 10.96 |
| | 4 | 1380 | 80.040 | 11.08 |
| | 5 | 1391 | 66.792 | 9.18 |
| Sal | 1 | 1374 | 81.432 | 11.32 |
| | 2 | 1381 | 81.432 | 11.26 |
| | 3 | 1354 | 64.584 | 9.10 |
| | 4 | 1362 | 81.432 | 11.42 |
| | 5 | 1364 | 81.432 | 9.04 |
| Sheesham | 1 | 1365 | 101.200 | 14.16 |
| | 2 | 1370 | 81.430 | 11.36 |
| | 3 | 1355 | 81.430 | 11.48 |
| | 4 | 1362 | 81.430 | 11.42 |
| | 5 | 1374 | 101.210 | 14.06 |

cutting. Hence, it was used further in analysis and optimization. A low value of feed was used for the case of aluminum as cutting at such high feeds was not possible with the machine. This force was used for the structural analysis of machine before and after optimization. The cutting force data that was obtained from the experiments was analyzed using the line diagram as shown in Fig. 5.

**Table 9** Cutting forces estimation for aluminium.

| Observation | Cutter speed (rpm) | Cutting power (W) | Cutting force (N) |
|---|---|---|---|
| 1 | 1350 | 179.800 | 25.44 |
| 2 | 1365 | 179.700 | 25.15 |
| 3 | 1352 | 179.800 | 25.34 |
| 4 | 1340 | 178.360 | 25.19 |
| 5 | 1358 | 179.800 | 25.28 |

It was found that the maximum cutting force variation was in the case of the tangential cutting of Sal wood. It was also observed that the cutting force variation was less in the radial direction for different observations of the given wood sample. The results of the maximum cutting force for the tangential and radial cutting are seen in Fig. 6. It was observed that the results for the radial cutting of both types of wood were found to be lower than tangential cutting. The maximum cutting force of all cases was found in aluminum.

### 3.2. Analysis of cutting force measuring machine

The analysis of the cutting force measuring machine was done for the case of static and dynamic loads. The force varies for different material samples; hence the maximum value of load obtained from the experimentation was used in the dynamic analysis. Whereas static loads, on the contrary, remains constant for all cases. Modal analysis was also performed on the finite element model to find the natural frequencies of the

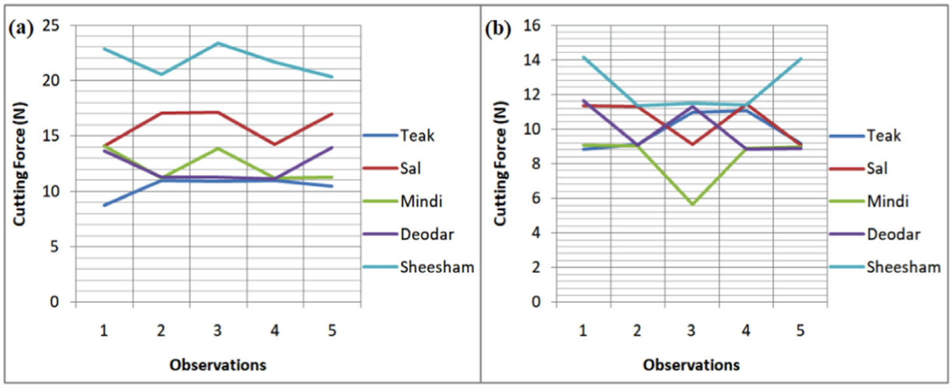


**Fig. 5** Cutting force diagram for (a) tangential and (b) radial cutting of various wood samples.

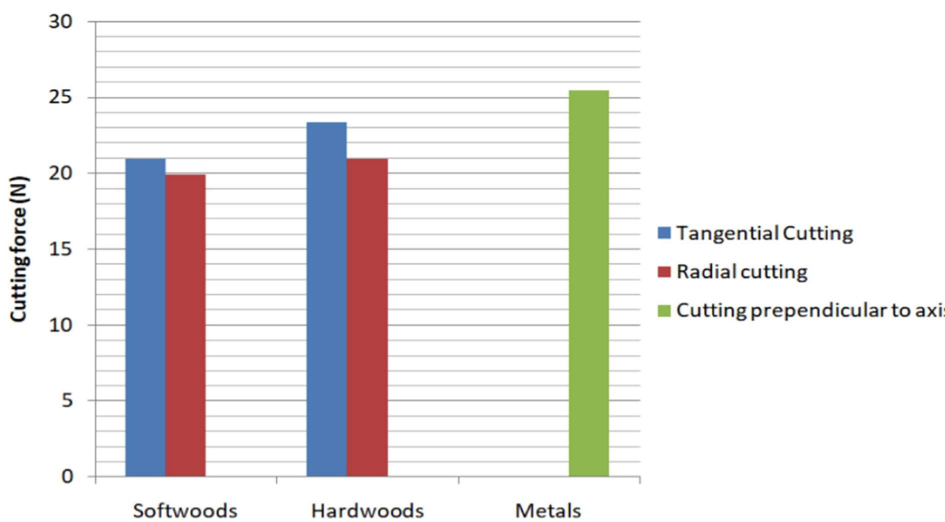


**Fig. 6** Maximum cutting force for different directions of the different categories of samples.

machine tool. Fig. 7 gives the Von-Mises stress results for the static and dynamic analysis of the cutting force measuring machine.

It was found that the stresses due to the static loads were much higher in comparison to the dynamic loads. It is due to larger value of maximum load in static condition i.e.,

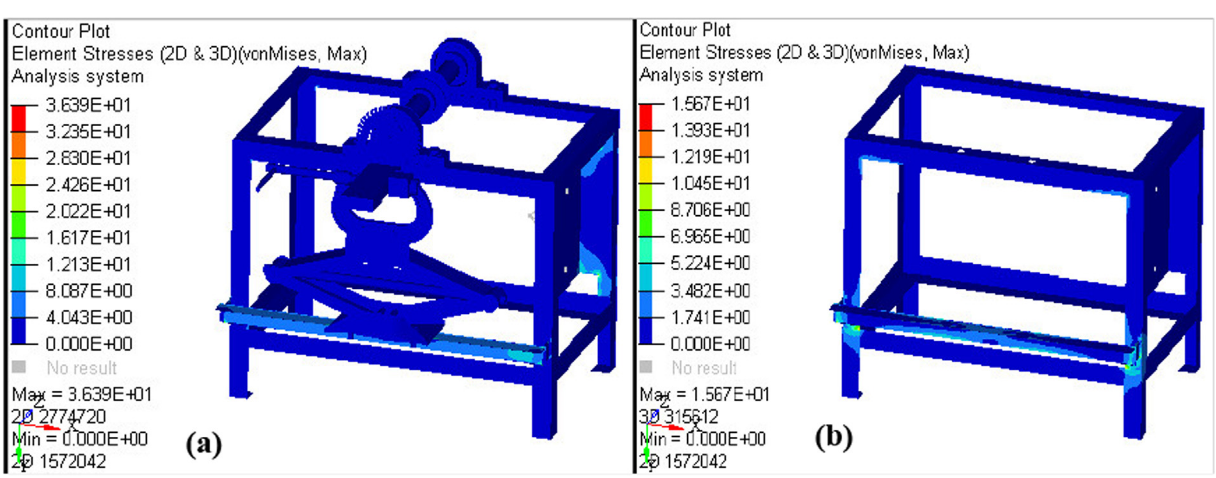


**Fig. 7** Von-Mises stress results for (a) static and (b) dynamic analysis of cutting force measuring machine.

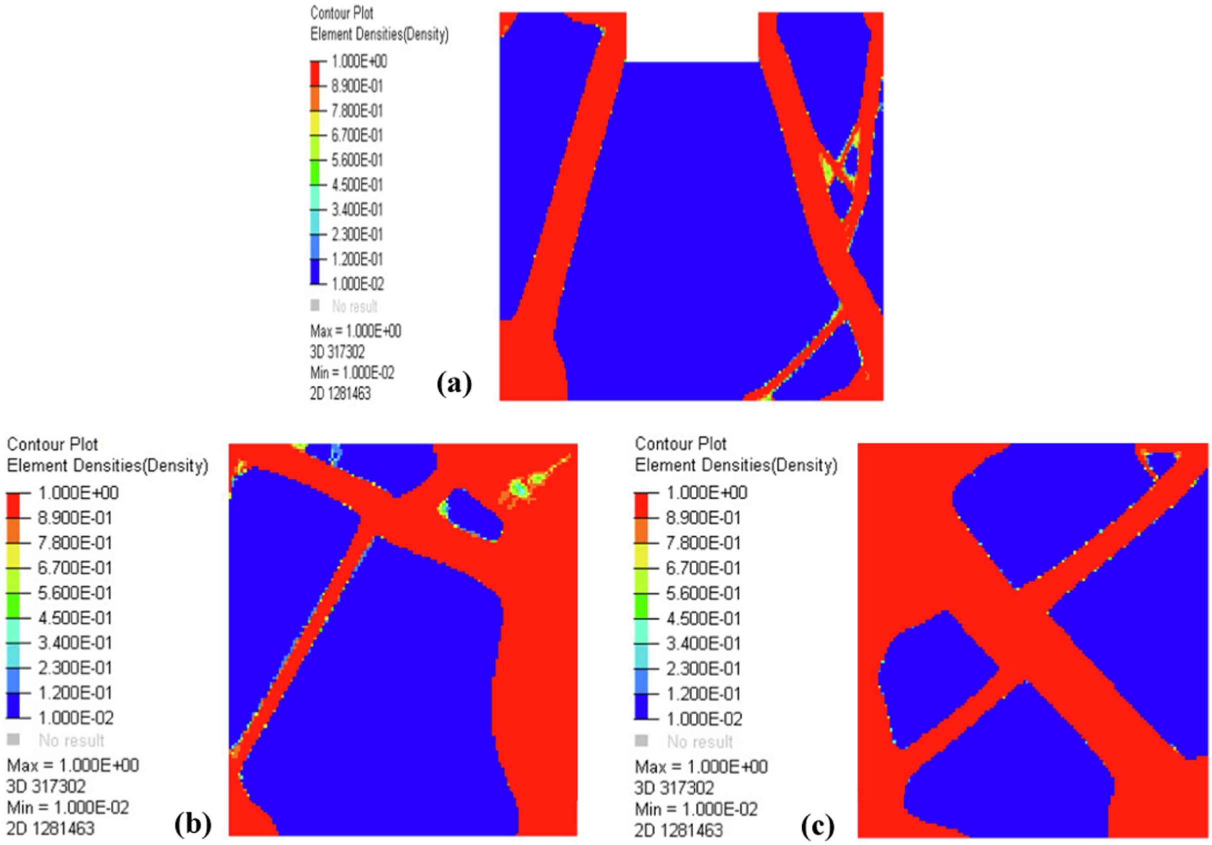


**Fig. 8** Density plot (a) Front, (b) Left and (c) Right views of cutting force measuring machine after topology optimization.

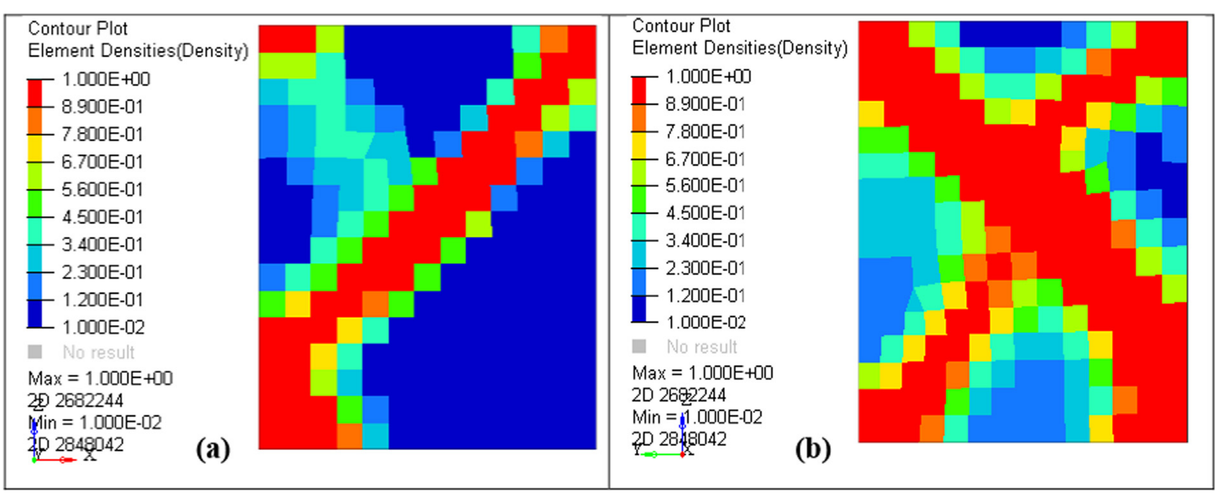


**Fig. 9** Density plot (a) Top, (b) Left views of cutting force measuring machine after topology optimization near left support of scissor jack.

35.28 N as compared to dynamic load of 25.44 N. Also, in the previous case the load is concentrated at point and in the latter; it is distributed over cutter perimeter [56]. The maximum stress was found near the motor mounting location in case of the static analysis and near the right end of the scissor jack support beam when looking from the front in the case of the dynamic analysis.

### *3.3. Topology optimization*

Topology optimization of machine tool structure was used to improve the behavior of machine tool. Although a minimum member size of 25 mm was used, members with dimension considerably less than the given value were also obtained. These members are essential for the load transmission to constrained

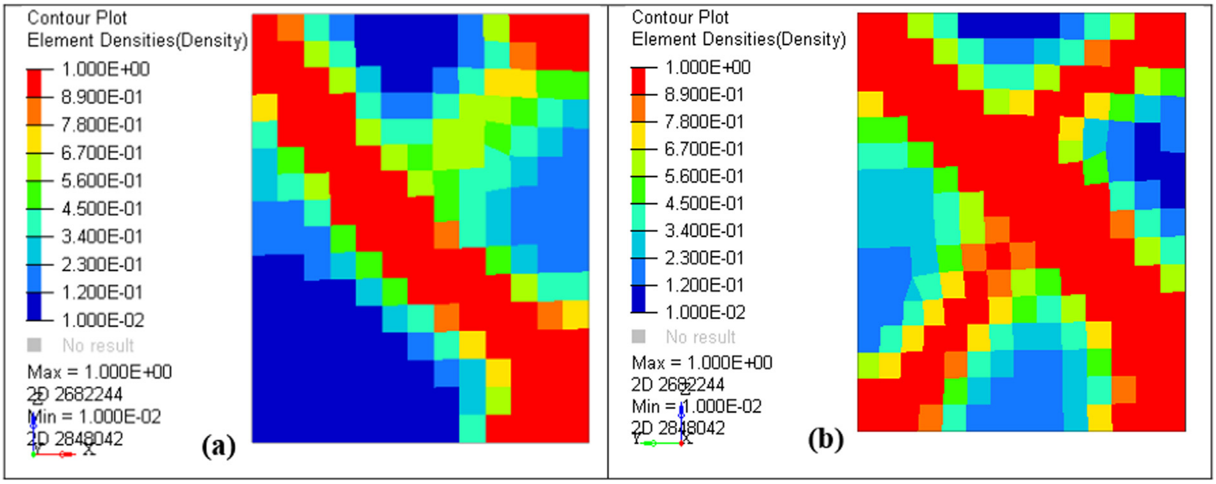


**Fig. 10** Density plot (a) Top, (b) Right views of cutting force measuring machine after topology optimization near right support of scissor jack.

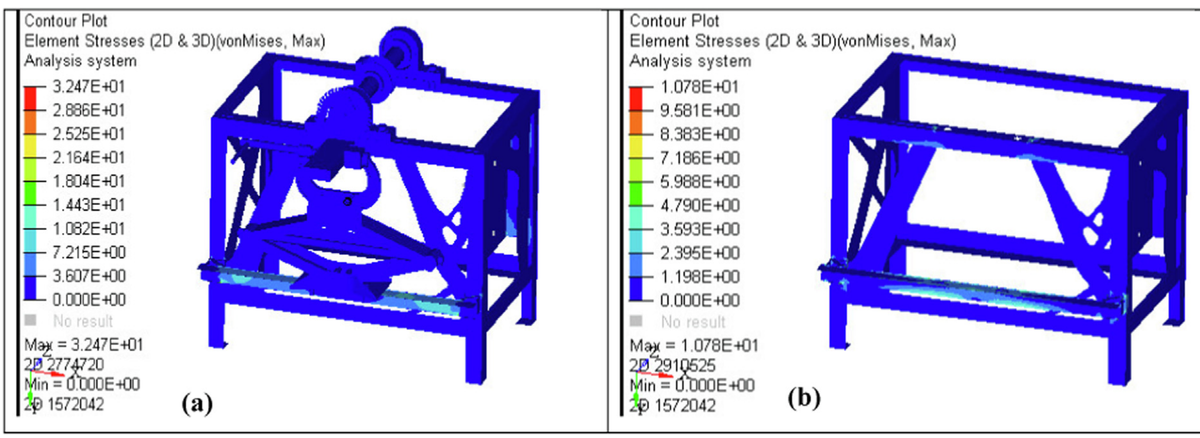


**Fig. 11** Von-mises stress results for (a) static and (b) dynamic analysis for optimized cutting force measuring machine.

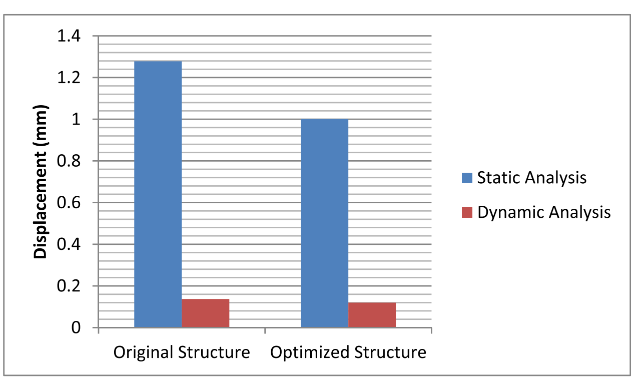


**Fig. 12** Displacement results for the static and dynamic analysis of the original and optimized structure.

location, hence were not completely eradicated. The mass of the structure after optimization was found out by multiplying the final volume by density. The mass of optimized part was found to be 1.93 kg. Figs. 8-10 shows the density plots for topology optimization of the stiffener plates of cutting force measuring machine.

**Table 10** Modal frequencies of the original and optimized structure.

| Mode | Original Structure (Hz) | Optimized Structure (Hz) | Increase in modal frequency (%) |
|---|---|---|---|
| 1 | 8.1 | 9.3 | 14.8 |
| 2 | 9.5 | 12.2 | 28.4 |
| 3 | 49.8 | 65.0 | 30.5 |
| 4 | 56.4 | 75.1 | 33.2 |
| 5 | 64.4 | 77.8 | 20.8 |

### *3.4. Reanalysis*

Reanalysis was done using similar loads and constraints to see improvement in the results of the analysis by the addition of the stiffener plates. The results that were obtained are shown in Fig. 11, which demonstrate a significant improvement in both the static and dynamic stress results.

The displacement results were also studied for the case of the static and dynamic analysis as shown in Fig. 12. The Fig. 12 shows decrease in the displacement for both static

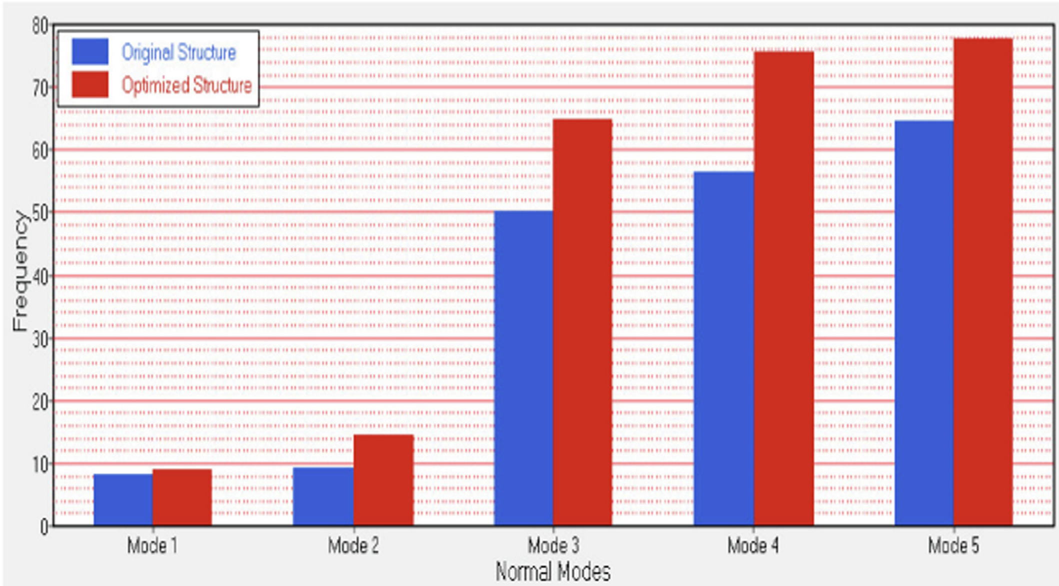


**Fig. 13** Comparison of modal frequencies of original and optimized structure.

and dynamic loading. The displacement for the case of the static loads was found to be 1.278 mm and 1.001 mm for original and optimized structures respectively. Also, for the dynamic loads, the values were found to be 0.01375 mm and 0.01202 mm for both the structures.

The results of the modal analysis are given in Table 10, which reveals that the constraints of the topology optimization problem have been satisfied. Here, first five modes of cutting machine were considered to see improvements in modal frequencies due to optimization.

A comparison was made between the modal frequencies of the original structure and optimized structure as shown in Fig. 13. There was a significant increase in modal frequency of third, fourth and fifth modes. However, there was not much difference in the first two modes.

## 4. Conclusions

The current study used FEM to examine the structural optimization of a machine tool. The issue of the structure's stability under the influence of the cutting force was found to be extremely crucial for obtaining machining accuracy. To begin the investigation, a machine tool structure was created and cutting forces for various samples of wood and Aluminum was estimated using the energy method. Hypermesh software was used to model the structure, while Optistruct was used for analysis and optimization. The initial structure was statically and dynamically analyzed, and value of maximum displacement and modal frequency were recorded. The structure than was optimized with the mass constraint fixed to 35 % of the initial volume using stiffener plates. The optimized structure was reanalyzed, and the maximum displacement was found to reduce by 21.6 % and 14.5 % for static and dynamic forces respectively. Moreover, the modal frequency of optimized structure was increased as compared with original structure by a maximum value of 33.2 %, thus increasing the gap with excitation frequency and hence will avoid condition of resonance. The study attempts to provide some insight into the optimization of the machine tool structure by using FEM technique to increase the stability of the machine tool structure by analyzing the location of stiffener plates to reduce overall weight.

## 5. Future scope and limitation of the study

The results are based on the element size and type, as the size of the element is reduced, the accuracy is increased and element type selected will also affects the result, but the factors like limitation of computer system configuration and optimization time should also be considered. Although in the study the average element size was kept 1.5 mm and the local mesh refinement was done to have stress results with accuracy of $\pm 0.001$ N/mm$^2$. The study can be improved by reducing the element size and increasing the number of nodes by selection of hire element type so that even a deflection in structure of micron can be detected and avoided to have ultra-precision work.

## Declaration of Competing Interest

The authors declare that they have no known competing financial interests or personal relationships that could have appeared to influence the work reported in this paper.

## References

[1] J. Wang, W. Niu, Y. Ma, L. Xue, H. Cun, Y. Nie, Y.D. Zhang, A CAD/CAE-integrated structural design framework for machine tools, Int. J. Adv. Manuf. Technol. 91 (2017) 545–568.
[2] N.S. Kalsi, R. Sehgal, V.S. Sharma, Cryogenic treatment of tool materials: a review, Mater. Manuf. Processes 25 (10) (2010) 1077–1100.
[3] M. Ebrahimi, R. Whalley, Analysis, modeling and simulation of stiffness in machine tool drives, Comput. Ind. Eng. 38 (2000) 93–105.

[4] D.-Y. Huang, J.-J. Lee, On obtaining machine tool stiffness by CAE techniques, Int. J. Mach. Tools Manuf 41 (8) (2001) 1149–1163.

[5] H. Shin, S. Kim, J. Jeong, J. Kim, Stiffness enhancement of a redundantly actuated parallel machine tool by dual support rims, Int. J. Precis. Eng. Manuf. 13 (9) (2012) 1539–1547.

[6] S. Saini, I.S. Ahuja, V.S. Sharma, Influence of cutting parameters on tool wear and surface roughness in hard turning of AISI H11 tool steel using ceramic tools, Int. J. Precis. Eng. Manuf. 13 (2012) 1295–1302.

[7] S. Murugan, P.R. Thyla, Mechanical and dynamic properties of alternate materials for machine tool structures: a review, J. Reinf. Plast. Compos. 37 (24) (2018) 1456–1467.

[8] D.G. Lee, J.D. Suh, H.S. Kim, J.M. Kim, Design and manufacture of composite high speed machine tool structures, Compos. Sci. Technol. 64 (2004) 1523–1530.

[9] Y. Altintas, C. Brecher, M. Weck, S. Witt, Virtual machine tool, CIRP Ann. 54 (2005) 115–138.

[10] D. Kono, T. Lorenzer, S. Weikert, K. Wegener, Evaluation of modelling approaches for machine tool design, Precis. Eng. 34 (2010) 399–407.

[11] Y. Meng, J. Wei, J. Wei, H. Chen, Y. Cui, An ANSYS/LS-DYNA simulation and experimental study of circular saw blade cutting system of mulberry cutting machine, Comput. Electron. Agric. 157 (2019) 38–48.

[12] W. Hu, H. Wan, H. Guan, Size effect on the elastic mechanical properties of beech and its application in finite element analysis of wood structures, Forests 10 (2019) 783.

[13] T. Krenke, S. Frybort, U. Müller, Cutting force analysis of a linear cutting process of spruce, Wood Mat. Sci. Eng. 13 (2018) 279–285.

[14] A.C. Nguyen, P. Vestartas, Y. Weinand, Design framework for the structural analysis of free-form timber plate structures using wood-wood connections, Autom. Constr. 107 (2019) 102948.

[15] T. Xiaoguang, R. Xiaozhong, G.R. Sai, W. Ya-hui, W. Xiao-bo, Lightweight optimization design of horizontal double-sided combined machine tool bed based on ansys workbench, Acad. J. Manuf. Eng. 17 (2019) 91–100.

[16] D. Dimitrov, S.D. Slavov, K. Yordanov, Stiffness design of machine tools structures by topology management optimization approach, IOP Conf. Ser.: Mater. Sci. Eng. 564 (2019) 012071.

[17] Z. Pandilov, V. Dukovski, Static and dynamic stiffness of the mechatronic position servo systems, Appl. Mech. Mater. 332 (2013) 186–193.

[18] H.-C. Moehring, C. Brecher, E. Abele, J. Fleischer, F. Bleicher, Materials in machine tool structures, CIRP Ann. 64 (2015) 725–748.

[19] M. Gupta, C. Goswami, N. Khandelwal, Design and structural analysis of 3-sided and 4-sided columns of a CNC machine using finite element analysis, Mater. Today:. Proc. 47 (2021) 5895–5900.

[20] L. Harzheim, G. Graf, A review of optimization of cast parts using topology optimization: II-Topology optimization with manufacturing constraints, Struct. Multidiscip. Optim. 31 (5) (2006) 388–399.

[21] M. Seabra, J. Azevedo, A. Araújo, L. Reis, E. Pinto, N. Alves, R. Santos, J.P. Mortágua, Selective laser melting (SLM) and topology optimization for lighter aerospace componentes, Procedia Struct. Integrity 1 (2016) 289–296.

[22] G.Y. Jeong, M.J. Park, Evaluate orthotropic properties of wood using digital image correlation, Constr. Build. Mater. 113 (2016) 864–869.

[23] A. Naylor, Evaluating the cutting mechanics of woodworking hand-saw teeth, Int. J. Mater. Mech. Manuf. 2 (2014) 113–116.

[24] G. Goli, M. Fioravanti, R. Marchal, L. Uzielli, S. Busoni, Up-milling and down-milling wood with different grain orientations-the cutting forces behaviour, Eur. J. Wood Wood Prod. 68 (2010) 385–395.

[25] J. Kováč, M. Mikleš, Research on individual parameters for cutting power of woodcutting process by circular saws, J. Forest Sci. 56 (2010) 271–277.

[26] H. Aknouche, A. Outahyon, C. Nouveau, R. Marchal, A. Zerizer, J.C. Butaud, Tool wear effect on cutting forces: in routing process of Aleppo pine wood, J. Mater. Process. Technol. 209 (6) (2009) 2918–2922.

[27] B. Goel, S. Singh, R.G.V. Sarepaka, V. Mishra, N. Khatri, V. Aggarwal, K. Nand, R. Kumar, Diamond turning of optical materials: a review, Int. J. Mach. Mach. Mater. 23 (2021) 160–190.

[28] F. Eyma, P.J. Méausoone, P. Martin, Strains and cutting forces involved in the solid wood rotating cutting process, J. Mater. Process. Technol. 148 (2004) 220–225.

[29] K.S.R.B. Malleswara, Design and structural analysis of CNC vertical milling machine bed address for correspondence, Int. J. Adv. Eng. Technol. 3 (2012) 97–100.

[30] L. Sun, S. Yang, P. Zhao, P. Wu, X. Long, Z. Jiang, Dynamic and static analysis of the key vertical parts of a large scale ultraprecision optical aspherical machine tool, Procedia CIRP 27 (2015) 247–253.

[31] H. Tiismus, A. Kallaste, T. Vaimann, A. Rassõlkin, State of the art of additively manufactured electromagnetic materials for topology optimized electrical machines, Addit. Manuf. 24 (2022) 102778.

[32] H. Yang, R. Zhao, W. Li, C. Yang, L. Zhen, Static and dynamic characteristics modeling for CK61125 CNC lathe bed basing on FEM, Procedia Eng. 174 (2017) 489–496.

[33] S.S. Abuthakeer, P.V. Mohanram, G. Mohankumar, Static and dynamic performance improvement of conventional computer numerical control machine tool bed with hybrid welded steel, Am. J. Appl. Sci. 8 (2011) 610–616.

[34] P. Bhambhatt, P., Surani, D.P., Patel, A.J., Patel, S.N. Chaudhari. Design and analysis of base structure of CNC router, J. Emerg. Technol. Innovative Res. 4 (2017) 242–247.

[35] R. Cazacu, L. Grama, Overview of structural topology optimization methods for plane and solid structures, Ann. ORADEA Univ. Fascicle Manag. Technol. Eng. 23 (2014) 1583–1591.

[36] S. Thapa, Structural design of 3-axis cnc machine tool for wood carving, Master of Engineering, 2014.

[37] M. Zhou, N. Pagaldipti, H.L. Thomas, Y.K. Shyy, An integrated approach to topology, sizing, and shape optimization, Struct. Multidiscip. Optim. 26 (5) (2004) 308–317.

[38] J. Liu, A.T. Gaynor, S. Chen, Z. Kang, K. Suresh, A. Takezawa, L. Li, J. Kato, J. Tang, C.C.L. Wang, L. Cheng, X. Liang, A.C. To, Current and future trends in topology optimization for additive manufacturing, Struct. Multidiscip. Optim. 57 (2018) 2457–2483.

[39] S. Lee, H. Kim, Q.X. Lieu, J. Lee, CNN-based image recognition for topology optimization, Knowledge-Based System 198 (2020) 105887.

[40] Z. Fan, L. Xia, W. Lai, Q. Xia, T. Shi, Evolutionary topology optimization of continuum structures with stress constraints, Struct. Multidiscip. Optim. 59 (2019) 647–658.

[41] Y. Saadlaoui, J.L. Milan, J.M. Rossi, P. Chabrand, Topology optimization and additive manufacturing: Comparison of conception methods using industrial codes, J. Manuf. Syst. 43 (2017) 178–186.

[42] P.H.L. Fernando, G.A. Santos, F.Y. Nakamoto, Topology optimization vehicle chassis: Software applied to optimization trucks and buses chassis stringer in automotive industry, EngOpt 2016–5th Int. Conf Eng. Optim. (2016) 1–12, https://doi.org/10.1142/9789812792259_0001.

[43] S. Junk, B. Klerch, L. Nasdala, U. Hochberg, Topology optimization for additive manufacturing using a component of a humanoid robot, Procedia CIRP 70 (2018) 102–107.

[44] J. Liu, Y. Ma, A survey of manufacturing oriented topology optimization methods, Adv. Eng. Softw. 100 (2016) 161–175.
[45] K.D. Tsavdaridis, J.J. Kingman, V.V. Toropov, Application of structural topology optimisation to perforated steel beams, Comput. Struct. 158 (2015) 108–123.
[46] M. Abdalmagid, E. Sayed, M. Bakr, A. Emadi, Geometry and topology optimization of switched reluctance machines: a review, IEEE Access 10 (2022) 5141–5170.
[47] S.L. Vatanabe, T.N. Lippi, C.R.D. Lima, G.H. Paulino, E.C.N. Silva, Topology optimization with manufacturing constraints: a unified projection-based approach, Adv. Eng. Softw. 100 (2016) 97–112.
[48] F. Mezzadri, V. Bouriakov, X. Qian, Topology optimization of self-supporting support structures for additive manufacturing, Addit. Manuf. 21 (2018) 666–682.
[49] J.H. Zhu, K.-K. Yang, W. Zhang, Backbone cup-a structure design competition based on topology optimization and 3D printing, Int. J. Simul. Multi. Des. Optim. 7 (2016) A1.
[50] Y. Liao, B. Liao, Dynamics modeling and modal analysis of machine tool considering joints parameters, Manuf. Technol. 19 (2019) 267–272.
[51] A. Ukil, R. Bloch, A. Andenna, Estimation of induction motor operating power factor from measured current and manufacturer data, IEEE Trans. Energy Convers. 26 (2011) 699–706.
[52] J.R. Wells, B.M. Nee, M. Amrhein, P.T. Krein, P.L. Chapman, Low-cost single-phase powered induction machine drive for residential applications, Conf. Proc. - IEEE Appl. Power Electron. Conf. Expo.-APEC 3 (2004) 1579–1583, https://doi.org/10.1109/apec.2004.1296075.
[53] S. Baloch, M.A. Mahar, R. Haider, S. Ahmed, Power factor improvement of AC-DC converter based on separately excited DC motor using passive filter, Open J. Energy Efficiency 5 (2016) 71–77.
[54] N.R. Tikhe, D.R. Tutakne, Single phase induction motor control with improved power factor using single switch, Int. J. Sci. Dev. Res. 2 (2017) 309–311.
[55] C.M. Burt, X. Piao, F. Gaudi, B. Busch, N.F.N. Taufik, Electric motor efficiency under variable frequencies and loads, J. Irrig. Drain. Eng. 134 (2008) 129–136.
[56] R. Singh, R. Kumar, A. Mishra, A. Agarwal, Structural analysis of Quadcopter frame, Mater. Today:. Proc. 22 (2020) 3320–3329.